Nanoscale Res Lett (2009) 4:39–46
DOI 10.1007/s11671-008-9199-0

NANO EXPRESS

In situ Polymerization of Multi-Walled Carbon Nanotube/Nylon-6 Nanocomposites and Their Electrospun Nanofibers

Khalid Saeed · Soo-Young Park · Sajjad Haider · Jong-Beom Baek

Received: 7 October 2008 / Accepted: 23 October 2008 / Published online: 18 November 2008

Abstract Multiwalled carbon nanotube/nylon-6 nanocomposites (MWNT/nylon-6) were prepared by in situ polymerization, whereby functionalized MWNTs (F-MWNTs) and pristine MWNTs (P-MWNTs) were used as reinforcing materials. The F-MWNTs were functionalized by Friedel-Crafts acylation, which introduced aromatic amine (COC_6H_4-NH_2) groups onto the side wall. Scanning electron microscopy (SEM) images obtained from the fractured surfaces of the nanocomposites showed that the F-MWNTs in the nylon-6 matrix were well dispersed as compared to those of the P-MWNTs. Both nanocomposites could be electrospun into nanofibers in which the MWNTs were embedded and oriented along the nanofiber axis, as confirmed by transmission electron microscopy. The specific strength and modulus of the MWNTs-reinforced nanofibers increased as compared to those of the neat nylon-6 nanofibers. The crystal structure of the nylon-6 in the MWNT/nylon-6 nanofibers was mostly γ-phase, although that of the MWNT/nylon-6 films, which were prepared by hot-pressing the pellets between two aluminum plates and then quenching them in icy water, was mostly α-phase, indicating that the shear force during electrospinning might favor the γ-phase, similarly to the conventional fiber spinning.

K. Saeed · S.-Y. Park (✉) · S. Haider
Department of Polymer Science, Kyungpook National University, #1370 Sankyuk-dong, Buk-gu, Daegu 702-701, South Korea
e-mail: psy@knu.ac.kr

J.-B. Baek
School of Chemical Engineering, Chungbuk National University, #12, Gaeshin, Heungduk, Cheongju, Chungbuk 361-763, South Korea

Keywords In situ polymerization · Nylon-6 · Nanofibers · Carbon nanotube · Nanocomposite

Introduction

Electrospinning is a process that can produce polymer nanofibers with diameters ranging from nanometer to submicrometers. The non-woven mats obtained from the electrospun nanofibers show a number of interesting characteristics such as high porosity, large surface area per unit mass, high gas permeability, and small inter-fibrous pore size. These properties qualify non-woven mats for a number of applications such as scaffolds in tissue engineering [1], electrically conductive nanofiber [2], drug delivery systems [3], nanofibrous membranes for fine filtration [4], and protective clothing [5]. During an electrospinning process, a high voltage is applied to a polymer solution or melt between a needle-tip and a metallic collector. The accumulated charges on the surface of droplet destabilize the partially hemispherical shape of the droplet, which converts into a Taylor's cone when the electric field is increased [6]. When the voltage reaches a critical value, the electric forces overcome the surface tension on the droplet and a jet of ultra-fine fibers is produced from the tip of the Taylor cone. The nanofibers of various polymers such as polyurethane [7], poly(*p*-phenylene terephthalamide) [8], polycaprolactone [9], nylon-6 [10], gelatin [11], polystyrene [12], polyaniline/polyethylene oxide blends [13], etc., have been prepared by using an electrospinning process.

Carbon nanotubes (CNTs) possess unique mechanical and optical properties, and excellent electrical and thermal conductivities along with chemical stability [14, 15]. Many researchers have focused on utilizing these

remarkable characteristics for engineering applications such as hydrogen storage, polymeric composites, [16], actuators [17, 18], chemical sensors [19], nanoelectronic devices [20], etc. The electrical, mechanical, and physical properties of the polymeric materials can be improved by incorporating a minute amount of CNTs. The dispersion and alignment of CNTs, however, have been problematic for these applications because CNTs are present in the form of bundles and ropes due to long-range lateral van der Waals interactions. Several approaches, such as chemical functionalization [21], wrapping [22], etc., have been used to obtain a good dispersion. However, chemical modification approaches have become popular. Introduction of organic pendants as molecular wedges onto the surface of CNTs could promote isolation. Thus, not only homogeneous dispersion can be achieved by breaking the close lateral contact between CNTs but also the chemical affinity of CNTs to organic matrices such as solvents and/or polymers can be enhanced. CNTs are, however, generally inert and stable against chemical reaction. Covalent modification of CNTs requires harsh reaction conditions in superacids, which are known to significantly damage CNTs. To resolve the issue on homogeneous dispersion of CNTs, the efficient and more or less destructive chemical modification of CNTs would be the best option [23]. The aligned CNTs have been synthesized by the deposition of CNTs onto the chemically modified substrate [24]. The electrospinning technique has recently been used to align CNTs in nanofibers as well [25]. The nanofibers from various CNTs/polymer nanocomposites (such as MWNT/polycaprolactone [26], MWNT/polyacrylonitrile [27], MWNT/polycarbonate [28], MWNT/polyethyleneoxide and MWNT/polyvinylalcohol [29], and SWNT/polystyrene, and SWNT/polyurethane [30]) were also prepared by electrospinning. Jose et al. [31] prepared the MWNT/nylon-6 nanofibers with acid-treated MWNTs, and studied the effect of collector speed on the morphologies of the nanofibers and the crystal structures of the nylon-6.

In the present study, we employed the aromatic amine functionalized multi-walled nanotubes (F-MWNTs) and an in situ polymerization method for the preparation of well-dispersed nanocomposites and nanofibers. The F-MWNT was functionalized by Friedel-Crafts acylation reaction in polyphosphoric acid (PPA) with phosphorous pentoxide (P_2O_5) as a drying reagent. PPA is known to be milder and much less corrosive than super acid media such as sulfuric and nitric acids which are known to damage CNTs [32, 33]. The mechanical properties, crystal structures, and morphologies of the F-MWNT/nylon-6 nanofibers were compared with those of pristine MWNTs (P-MWNT)/nylon-6 nanofibers in this work.

Materials and Methods

Materials

ε-Caprolactam (99% purity) and 6-aminocaproic acid (6-amino hexanoic acid) (99% purity) were purchased from Aldrich and Sigma, respectively, and used as received. Extra pure formic acid was purchased from Duksan chemicals. The MWNTs (CVD MWNTs, 95 vol% purity), which were manufactured by thermal chemical vapor deposition, were supplied by Nanomirea© [34]. The diameter and length of the CVD MWNTs were 20–40 nm and 30–40 μm, respectively.

Functionalization of MWNTs

The F-MWNTs were prepared by Friedel-Crafts acylation as shown in Scheme 1 [35, 36]. *p*-Amino benzoic acid, P-MWNTs, and PPA were placed in resin flask equipped with a mechanical stirrer, and nitrogen inlet and outlet. The mixture was heated to 130 °C for 3 h, and P_2O_5 was then added into it. The reaction was run for an additional 12 h at 130 °C, after which the mixture was cooled and diluted with water. The precipitates were collected and washed with ammonium hydroxide. The F-MWNTs were Soxhlet-extracted with water for 72 h to remove PPA, unreacted *p*-amino benzoic acid and methanol, and were finally dried under a reduced pressure for 3 days at 100 °C.

In situ Polymerization of the Nanocomposites

In situ polymerization of ε-caprolactam in the presence of F-MWNTs (or P-MWNTs) was carried out to prepare the F-MWNT/nylon-6 and the P-MWNT/nylon-6, respectively (Scheme 2). The synthetic procedure for the P-MWNT/nylon-6 is as follows: a known weight % of P-MWNTs and 24 g of ε-caprolactam were placed in a three-neck round

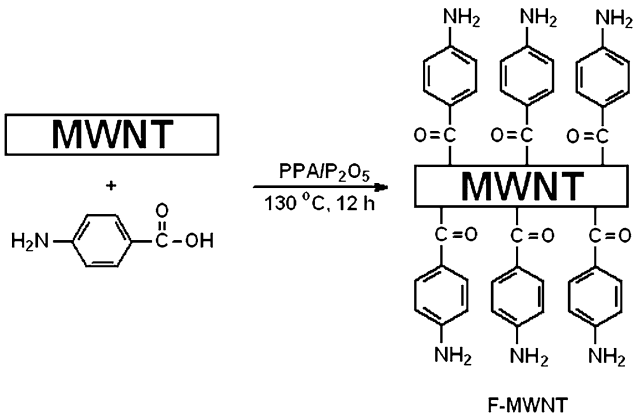

Scheme 1 Side-wall functionalization of MWNTs (F-MWNTs) by Friedel-Crafts acylation [33, 34]

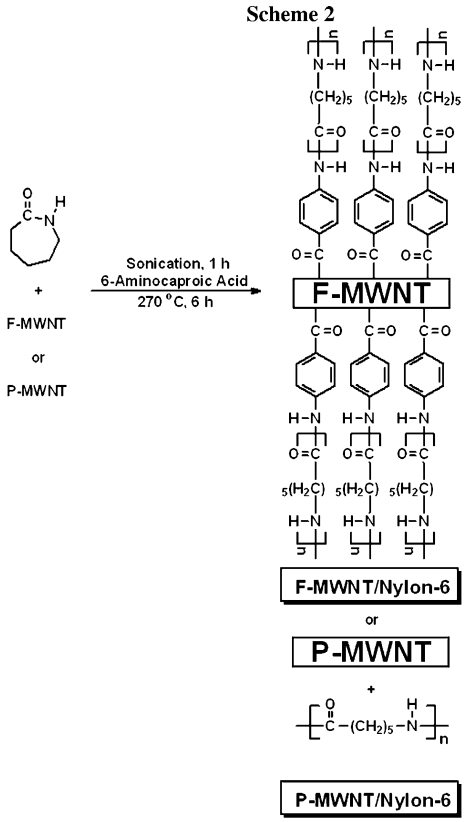

Scheme 2 In situ polymerizations of the F-MWNT/nylon-6 and the P-MWNT/nylon-6

bottom flask. The weight % of the input MWNT is denoted as ϕ in this article. The mixture was sonicated for 1 h at 120 °C to obtain a homogenous dispersion of the P-MWNTs in ε-caprolactam, and then 2.4 g of 6-amino-caproic acid were added to the suspension. The flask was transferred to a preheated oil bath (270 °C) and heated for 6 h with mechanical stirring under nitrogen atmosphere. The same procedure was used for the F-MWNT/nylon-6. The viscosity-average molecular weight of the synthesized nylon-6 was 19,000.

Electrospinning

The nylon-6, the F-MWNT/nylon-6, and the P-MWNT/nylon-6 were dissolved in formic acid [37]. The solutions of the composites were sonicated in formic acid for 1 h in order to accelerate homogeneous dispersion of the MWNTs. The prepared solutions were added to a 10 mL glass syringe using a needle tip with a 0.5 mm diameter. The feeding rate was 0.2 mL/h, which was controlled by a syringe pump. Electrospinning voltage, the distance between the needle tip and the collector, and the operating temperature were 15 kV, 12 cm, and 25 °C, respectively.

Characterization

FT-IR spectra were recorded using a JASCO FT/IR 620 spectrometer. The samples were mixed with KBr and pressed into 10 mm diameter pellets. The spectra were derived from 50 co-added interferograms, which were obtained at a resolution of 1 cm^{-1}. The SEM micrographs of the platinum-coated fractured surfaces (broken in the liquid nitrogen) were analyzed using a Hitachi S-570. Thermogravimetric analysis (TGA) thermograms were obtained in a nitrogen atmosphere at a heating rate of 20 °C/min between 25 and 900 °C using a TA4000/Auto DSC 2910 System. Melt viscosities were recorded on a UDS 200 Rheometer (Physica©). All samples (0.3 mm thick) were measured at 250 °C with an angular frequency range between 0.1 and 100 rad/s with a 5% strain. The measurements were conducted using cone and plate geometry with a 25 mm diameter and a one degree (1°) cone angle. The samples for transmission electron microscopy (TEM) were prepared by directly depositing the nanofibers onto the copper grids. The samples were analyzed using a Hitachi M-7600 with an accelerated voltage of 100 kV. The tensile properties were measured using an Instron (Model M 4465). The tests were carried out at room temperature with 30 mm gauge length and a 10 mm/min crosshead speed. The specific tensile strength and modulus were calculated because the pores in the cross section of the nanofiber mat do not give the true stress if the cross-sectional area is used for calculating the nominal stress. They were calculated by dividing the force by weight per length. The wide angle X-ray scattering (WAXS) patterns were recorded by using a Statton camera with 49 mm sample-to-detector distance. The two-dimensional X-ray patterns were integrated along the azimuthal direction in order to provide one-dimensional curves.

Results and Discussion

Functionalization of MWNTs

Functionalization of MWNTs was performed as indicated by literature procedure [33]. Figure 1 shows the FT-IR spectra of the P-MWNTs and the F-MWNTs. The P-MWNTs did not show any particular peaks while the F-MWNTs showed a N–H stretching band at 1600 cm^{-1}, indicating that functional groups were introduced [38]. This result demonstrates that 4-aminobenzoyl moiety was covalently attached to the surface of MWNT as shown in Scheme 1 [36]. The aromatic amine groups will provide the sites for the ring opening initiation of ε-caprolactam to afford the nylon-6 grafted F-MWNT nanocomposites (F-MWNT/nylon-6) (Scheme 2).

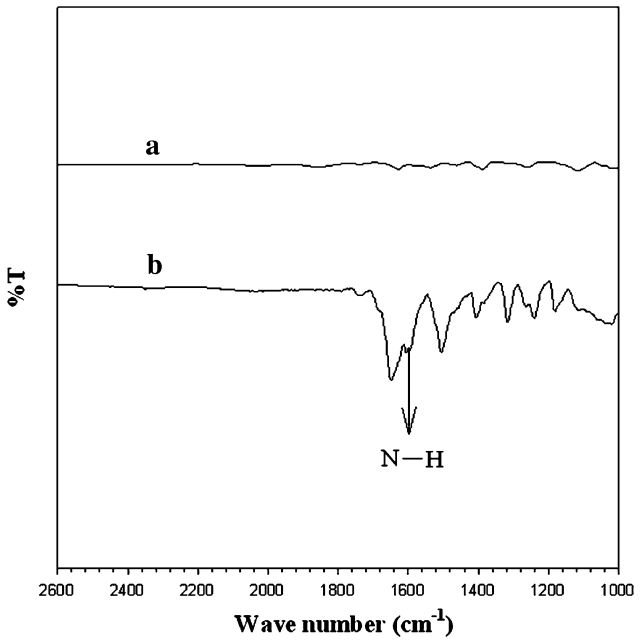

Fig. 1 FT-IR spectra of (a) P-MWNTs and (b) F-MWNTs

In situ Polymerization

In situ polymerization of ε-caprolactam in the presence of the F-MWNTs and the P-MWNTs was carried to prepare the F-MWNT/nylon-6 and the P-MWNT/nylon-6 as described in Scheme 2. Figure 2 represents the SEM micrographs of the fractured surfaces of the P-MWNT (5 wt%)/nylon-6 (Fig. 2a) and the F-MWNT (5 wt%)/nylon-6 (Fig. 2b). The F-MWNTs seemed to be better dispersed than the P-MWNTs in nylon-6 matrix. This better dispersion of MWNTs in the F-MWNT/nylon-6 might be due to chemical affinity originating from the chemical modification, which allowed MWNTs to be better compatible with nylon-6 [39, 40].

Thermal Properties

Figure 3 shows the TGA thermograms of the P-MWNTs, F-MWNTs, nylon-6, P-MWNT (5 wt%)/nylon-6, and F-MWNT (5 wt%)/nylon-6. The onset temperature of weight loss of the P-MWNTs occurred at 600 °C while that of the F-MWNTs occurred at 460 °C. The early weight loss of the F-MWNTs could be attributed to the stripping off of aromatic amine moieties from the F-MWNTs. The pure nylon-6 started weight loss at ~400 °C and was completely decomposed at 500 °C. Both P-MWNT/nylon-6 and F-MWNT/nylon-6 were decomposed at ~500 °C and the residual amount was in good agreement with the input MWNT.

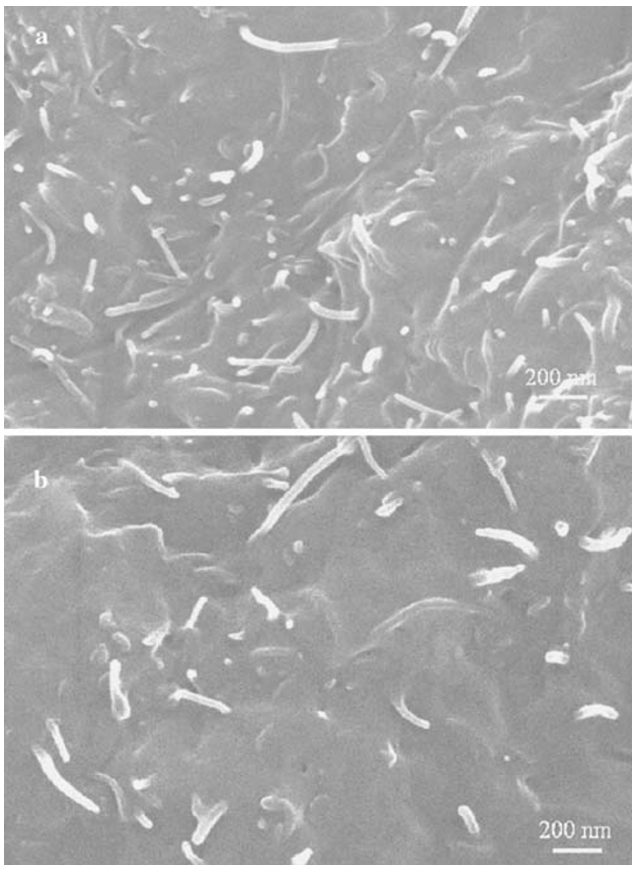

Fig. 2 SEM images of the fractured surfaces of **a** P-MWNT (5 wt%)/nylon-6 and **b** F-MWNT (5 wt%)/nylon-6

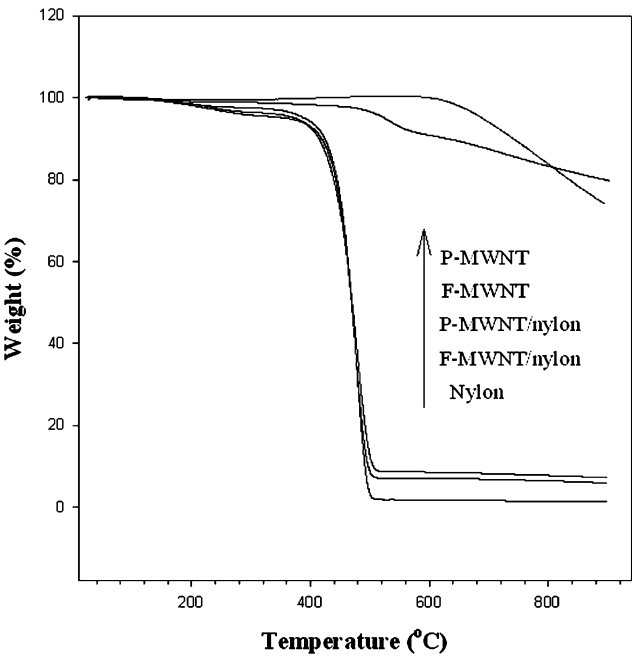

Fig. 3 TGA thermograms of P-MWNTs, F-MWNTs, nylon-6, P-MWNT (5 wt%)/nylon-6, and F-MWNT (5 wt%)/nylon-6

Melt Viscosities

Figure 4 displays the complex viscosities (η^*s) of the P-MWNT/nylon-6 (Fig. 4a) and the F-MWNT/nylon-6 (Fig. 4b) as a function of frequency. The η^*s at low frequencies (<1 rad/s) increased as the ϕ increased for both the P-MWNT/nylon-6 and the F-MWNT/nylon-6. The η^*s of the F-MWNT/nylon-6 and the P-MWNT/nylon-6 showed Newtonian behavior for low ϕ. Both composite systems showed profound shear-thinning behavior as the ϕ increased. Percolation threshold represents a starting point of a three-dimensional MWNT network in the matrix, and can be determined from the starting ϕ at which the viscosity does not show Newtonian but shear-thinning behavior. The percolation thresholds of the P-MWNT/nylon-6 and the F-MWNT/nylon-6 were 1 and 3 wt%, respectively [41–43]. These low values indicate that the MWNTs were dispersed well in the polymer matrix so the small amounts of the MWNTs were needed for the three-dimensional network.

SEM of Nanofibers

Figure 5 represents the SEM images of the F-MWNT/nylon-6 and the P-MWNT/nylon-6 nanofibers, which were electrospun from 25 wt% solutions. The diameters were in the range of 100 to 400 ± 50 nm. Beads were sometimes formed in the P-MWNT/nylon-6 nanofibers (Fig. 5d–f) while they were rarely observed in the F-MWNT/nylon-6 nanofibers (Fig. 5a–c). This might be due to the better dispersion of the MWNTs in the F-MWNT/nylon-6 than in the P-MWNT/nylon-6. Ra et al. [27] also observed that more beads were formed in the MWNT/PAN when the dispersion of the MWNTs was poor even at the low ϕs.

TEM of Nanofibers

Figure 6 shows the TEM micrographs of the MWNT/nylon-6 nanofibers. The individual MWNTs were embedded and were well dispersed in the nanofibers. Most MWNTs were well oriented along the fiber axes, although the orientation of the CNTs was known to be difficult to achieve by conventional mechanical drawing. The randomly oriented MWNTs were sometimes observed in the entangled, knotted and protruded forms but these instances were rare. Dror et al. [44] also observed such irregularities in the MWNT/PEO nanofibers.

Mechanical Properties of MWNT/Nylon-6 Nanofibers

The tensile properties of the nanofibers are given in Table 1. The specific tensile strengths of the F-MWNT (1 wt%)/nylon-6, the P-MWNT (1 wt%)/nylon-6, and the

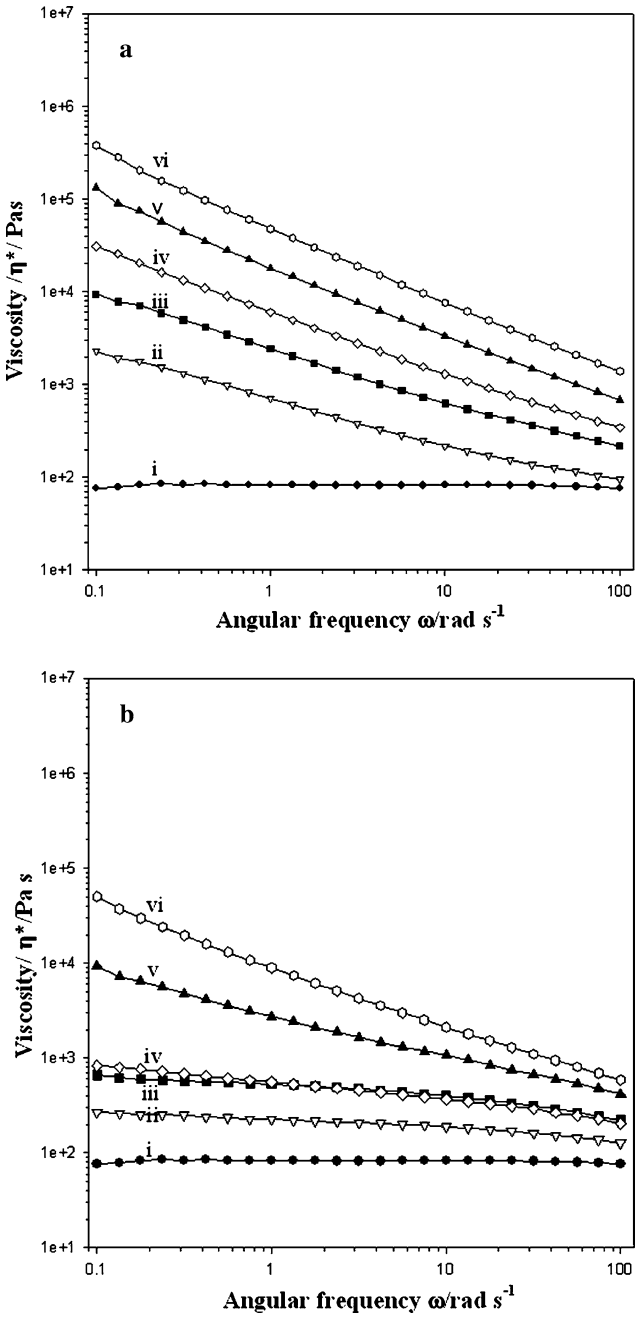

Fig. 4 Complex viscosities (η^*s) of **a** P-MWNT/nylon-6 and **b** F-MWNT/nylon-6 at ϕ = (i) 0, (ii) 1, (iii) 2, (iv) 3, (v) 5, (vi) 7

nylon-6 nanofibers were 389, 359 and 207 kgf cm/g, respectively, and the specific modulus of them were 295, 247, and 219 kgf cm/g, respectively. The specific tensile strength and modulus of MWNT/nylon-6 nanofibers were enhanced as compared to those of the nylon-6 nanofibers, although the elongation at break did not change significantly. The P-MWNT/nylon-6 nanofibers showed inferior mechanical properties to the F-MWNT/nylon-6 due to the poor dispersion of the P-MWNTs [45]. The bead formation might be another reason for the poor mechanical properties

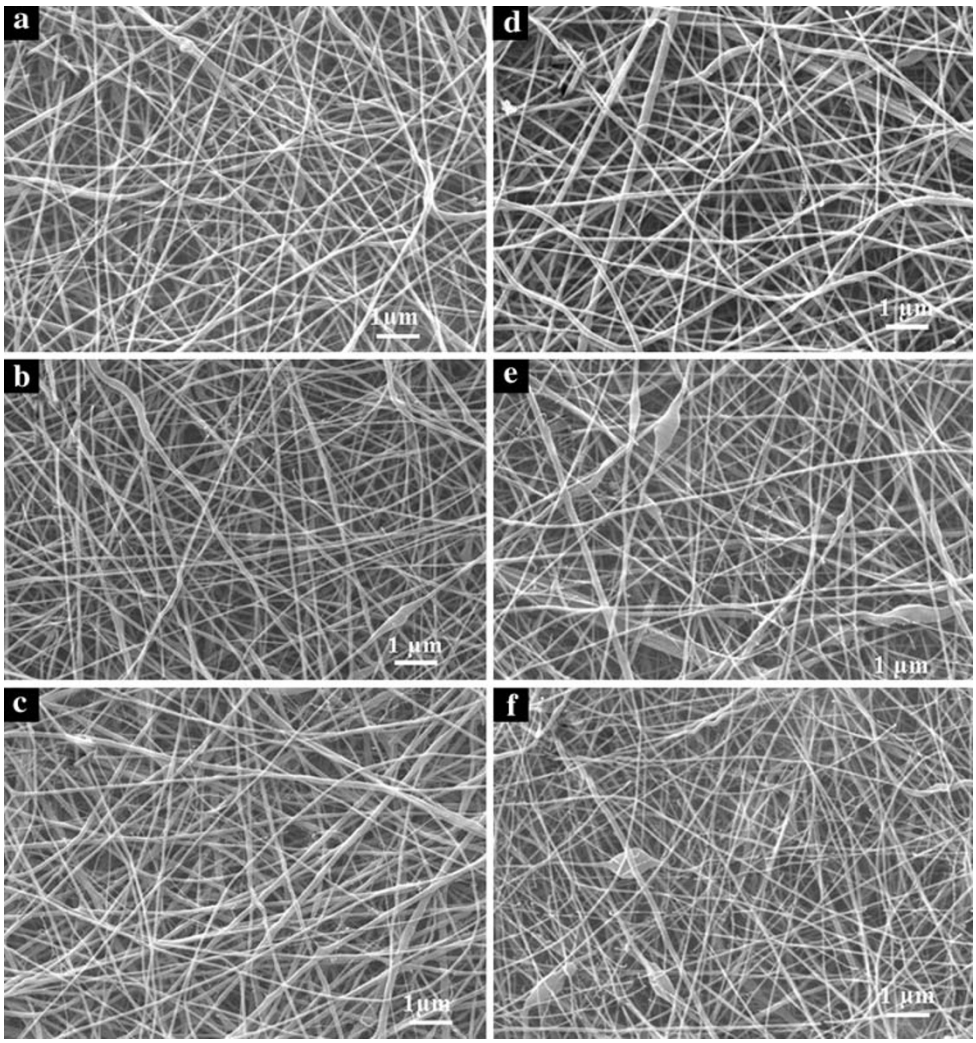

Fig. 5 SEM images of F-MWNT/nylon-6 (**a**–**c**) and P-MWNT/nylon-6 (**d**–**f**) nanofibers which were made from 25 wt% solutions at $\phi = 1$ (**a**, **d**), 2 (**b**, **e**), and 3 (**c**, **f**)

of the P-MWNT/nylon-6 nanofibers. Poor mechanical properties for the beaded nanofibers were also reported by Inai et al. [46].

Crystalline Structure

Figure 7a and b shows the WAXS patterns of the nanofibers and films respectively. The films were made by hot-pressing the pellets between two aluminum plates and then quenching them in icy water. Nylon-6 commonly exhibits two crystalline phases at room temperature, α and γ, where α is thermodynamically favored. The γ-phase is often associated with the formation of extended chain crystals and is typically obtained from a process involving elongational flow [47]. The reflections at 2θ = 11 and 21° are −201/200/001 and 020 of the γ form, respectively, and the reflections at $2\theta = \sim 20$ and 23° are 200 and 002 of the α form, respectively [47]. The nanocomposite nanofibers (Fig. 7a) have two characteristic γ-phase peaks (at $2\theta = \sim 11$ and 21°), although the nanocomposite films (Fig. 7b) show two characteristic α-phase peaks (at $2\theta = \sim 20$ and 23°). The observation of the γ-phase in the nanocomposite nanofibers might be due to the elongational flow during electrospinning because the γ-phase usually observed in the conventional fibers. The broad peaks of the WAXS patterns in the nanofibers were due to the small size of the crystal [48].

Conclusions

We prepared two kinds of the nanocomposites by using an in situ polymerization method in the presence of the F-MWNTs and the P-MWNTs. The F-MWNTs were functionalized by Friedel-Crafts acylation, which introduced aromatic amine (COC_6H_4-NH_2) groups onto the side wall, and the P-MWNTs were pristine MWNTs. The F-MWNTs were better dispersed in the nylon-6 matrix than the P-MWNTs as indicated by the low percolation threshold (1 wt%) in the rheological data and the SEM

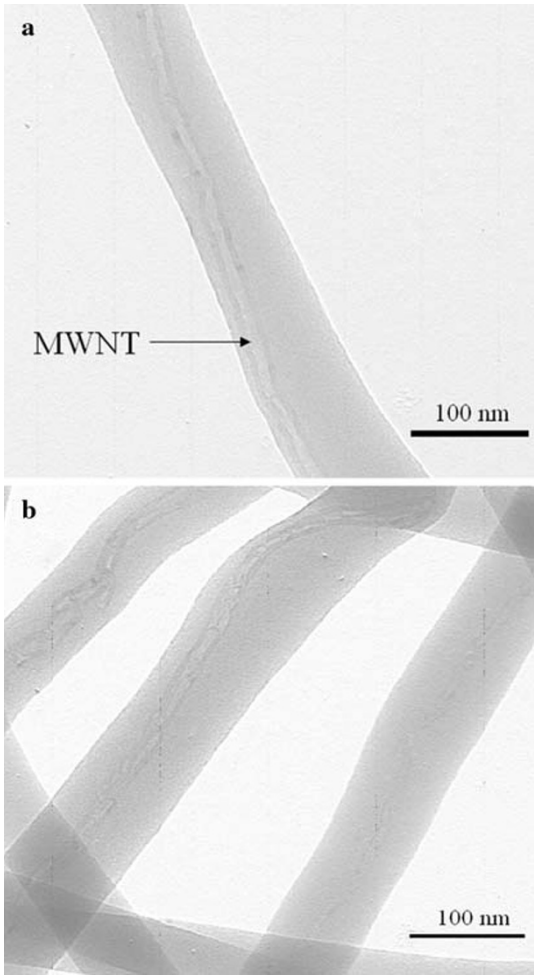

Fig. 6 TEM images of the nanofibers of **a** F-MWNT (2 wt%)/nylon-6 and **b** P-MWNT (2 wt%)/nylon-6

micrographs. The nanofibers were prepared from the nanocomposite solutions by an electrospinning method. The individual MWNTs were embedded within the nanofibers and well oriented along the fiber axes. The specific strength and modulus of nanocomposite nanofibers increased as compared to those of neat nylon-6 nanofibers. Nanocomposite nanofibers contained mostly γ-phase of nylon-6 while the nanocomposite films, which were prepared by hot-pressing the pellets between two aluminum

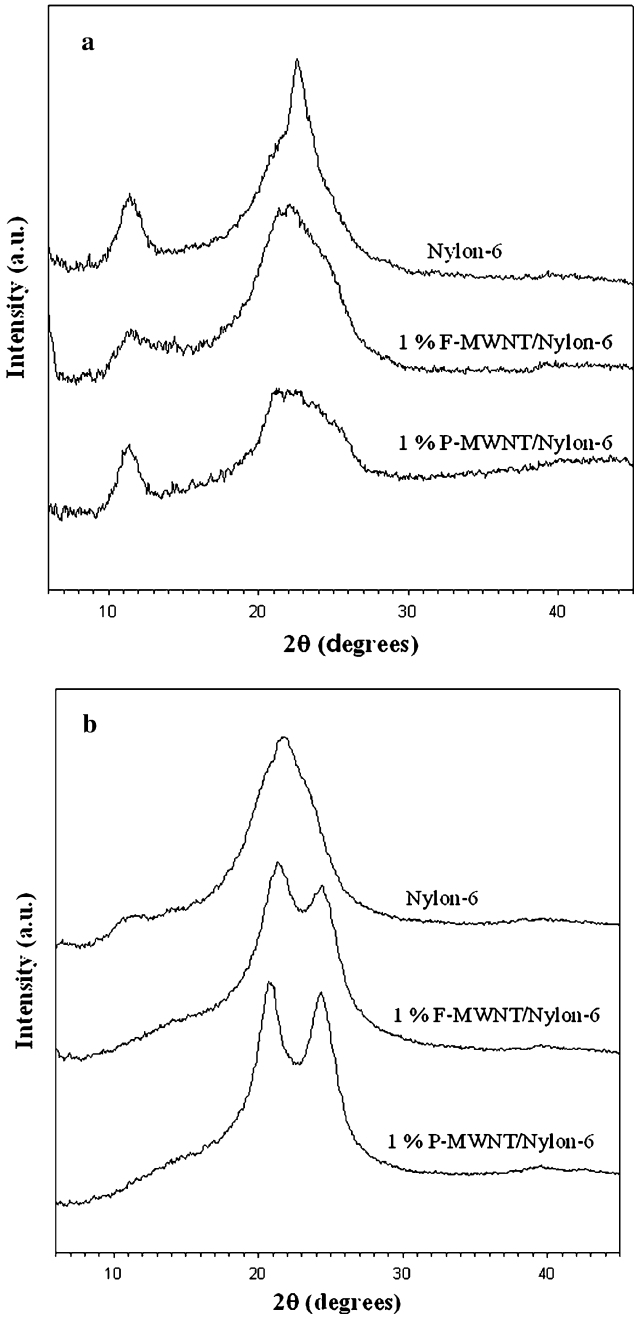

Fig. 7 WAXS patterns of **a** nanofibers and **b** films of nylon-6 and MWNT/nylon-6

Table 1 Mechanical properties of nylon-6 and MWNTs/nylon-6 nanofibers

Samples	Specific tensile strength (kgf cm/g)	Specific modulus (kgf cm/g)	Elongation at break (%)
Nylon-6	207.6 ± 41.7	219.1 ± 52.2	22.7 ± 4.9
F-MWNT (1 wt%)/nylon-6	389.1 ± 52.8	295.3 ± 40.2	24.7 ± 5.1
F-MWNT (2 wt%)/nylon-6	367.2 ± 65.6	312.5 ± 16.4	33.9 ± 14.9
P-MWNT (1 wt%)/nylon-6	359.2 ± 37.8	247.7 ± 43.7	22.5 ± 9.9
P-MWNT (2 wt%)/nylon-6	189.4 ± 41.2	118.8 ± 39.7	16.9 ± 1.8

plates and then quenching them in icy water, did mostly α-phases. This difference might be due to the shear stress during electrospinning.

Acknowledgement Financial support from Asian Office of Aerospace Research and Development through Air Force Research Laboratory is gratefully acknowledged.

References

1. C.J. Buchko, L.C. Chen, Y. Shen, D.C. Martin, Polymer (Guildf) **40**, 7397 (1999). doi:10.1016/S0032-3861(98)00866-0
2. A.G. MacDiarmid, W.E. Jones Jr., I.D. Norris, J.A. Gao, T. Johnson Jr., N.J. Pinto, J. Hone, B. Han, F.K. Ko, H. Okuzaki, M. Llaguno, Synth. Met. **119**, 27 (2001). doi:10.1016/S0379-6779(00)00597-X
3. E.-R. Kenawy, G.L. Bowlin, K. Mansfield, J. Layman, D.G. Simpson, E.H. Sanders, G.E. Wnek, J. Control. Release **81**, 57 (2002). doi:10.1016/S0168-3659(02)00041-X
4. P.W. Gibson, H.L. Schreuder-Gibson, D. Rivin, AIChE J. **45**, 190 (1999)
5. P. Gibson, H.L. Schreuder-Gibson, D. Rivin, Colloids Surf. A Physicochem. Eng. Asp. **187–188**, 469 (2001)
6. G.I. Taylor, Proc. R. Soc. Lond. A Math. Phys. Sci. **313**, 453 (1969). doi:10.1098/rspa.1969.0205
7. G. Srinivasan, D.H. Reneker, Polym. Int. **36**, 195 (1995). doi:10.1002/pi.1995.210360210
8. I.D. Cha, H.K. Kim, K.H. Lee, Y.C. Jung, J.W. Cho, B.C. Chun, J. Appl. Polym. Sci. **96**, 460 (2005). doi:10.1002/app.21467
9. C.-M. Hsu, S.N. Shivkumar, Macromol. Mater. Eng. **289**, 334 (2004). doi:10.1002/mame.200300224
10. Y.J. Ryu, H.Y. Kim, K.H. Lee, H.C. Park, D.R. Lee, Eur. Polym. J. **3**, 91883 (2003)
11. C.S. Ki, D.H. Baek, K.D. Gang, K.H. Lee, I.C. Um, Y.H. Park, Polymer (Guildf) **46**, 5094 (2005). doi:10.1016/j.polymer.2005.04.040
12. L. Wannatong, A. Sirivat, P. Supaphol, Polym. Int. **53**, 1851 (2004). doi:10.1002/pi.1599
13. P.K. Kahol, N.J. Pinto, Synth. Met. **140**, 269 (2004). doi:10.1016/S0379-6779(03)00370-9
14. S. Iijima, Nature **354**, 56 (1991). doi:10.1038/354056a0
15. E.W. Wong, P.E. Sheehan, C.M. Lieber, Science **277**, 1971 (1997). doi:10.1126/science.277.5334.1971
16. C. Liu, Y.Y. Fan, M. Liu, H.T. Cong, H.M. Cheng, M.S. Dresselhaus, Science **286**, 1127 (1999). doi:10.1126/science.286.5442.1127
17. R.H. Baughman, C. Cui, A.A. Zakhidov, Z. Iqbal, J.N. Barisci, G.M. Spinks, G.G. Wallace, A. Mazzoldi, D.D. Rossi, A.G. Rinzler, O. Jaschinski, S. Roth, M. Kertesz, Science **284**, 1340 (1999). doi:10.1126/science.284.5418.1340
18. S. Haider, S.-Y. Park, K. Saeed, B.L. Farmer, Sens. Actuators B Chem. **124**, 517 (2007). doi:10.1016/j.snb.2007.01.024
19. J. Kong, N.R. Franklin, C. Zhou, M.G. Chapline, S. Peng, K. Cho, H. Dai, Science **287**, 622 (2002). doi:10.1126/science.287.5453.622
20. S.J. Tans, A.R.M. Verschueren, C. Dekker, Nature **393**, 49 (1998). doi:10.1038/29954
21. M. Holzinger, O. Vostrowsky, A. Hirsch, F. Hennrich, M. Kappes, R. Weiss, F. Jellen, Angew. Chem. Int. Ed. Engl. **40**, 4002 (2001). doi:10.1002/1521-3773(20011105)40:21<4002::AID-ANIE4002>3.0.CO;2-8
22. A. Hirsch, Angew. Chem. Int. Ed. Engl. **41**, 1853 (2002). doi:10.1002/1521-3773(20020603)41:11<1853::AID-ANIE1853>3.0.CO;2-N
23. H.J. Lee, S.W. Han, Y.D. Kwon, L.S. Tan, J.B. Baek, Carbon **46**, 1850 (2008). doi:10.1016/j.carbon.2008.07.027
24. R.R. Schlittler, J.W. Seo, J.K. Gimzewski, C. Durkan, M.S.M. Saifullah, M.E. Welland, Science **292**, 1136 (2001). doi:10.1126/science.1057823
25. S. Kedem, J. Schmidt, Y. Paz, Y. Cohen, Langmuir **21**, 5600 (2005). doi:10.1021/la0502443
26. H. Zeng, C. Goa, D. Yan, Adv. Funct. Mater. **16**, 812 (2006). doi:10.1002/adfm.200500607
27. J.R. Ra, K.H. An, K.K. Kim, S.Y. Jeong, Y.H. Lee, Chem. Phys. Lett. **413**, 188 (2005). doi:10.1016/j.cplett.2005.07.061
28. G.-M. Kim, G.H. Michler, P. Potschk, Polymer (Guildf) **46**, 7346 (2005). doi:10.1016/j.polymer.2005.06.008
29. W. Zhou, Y. Wu, F. Wei, G. Lou, W. Qian, Polymer (Guildf) **46**, 12689 (2005). doi:10.1016/j.polymer.2005.10.114
30. R. Sen, B. Zhao, D. Perea, M.E. Itkis, H. Hu, J. Love, E. Bekyarova, R.C. Haddon, Nano Lett. **4**, 459 (2004). doi:10.1021/nl035135s
31. M.V. Jose, B.W. Steinert, V. Thomas, D.R. Dean, M.A. Abdalla, G. Price, G.M. Janowski, Polymer (Guildf) **48**, 1096 (2007). doi:10.1016/j.polymer.2006.12.023
32. J.-B. Baek, L.S. Tan, Polymer (Guildf) **44**, 4135 (2003). doi:10.1016/S0032-3861(03)00374-4
33. J.-B. Baek, S.-Y. Park, G.E. Price, C.B. Lyons, L.S. Tan, Polymer (Guildf) **46**, 1543 (2005). doi:10.1016/j.polymer.2004.12.022
34. http://www.nanomirea.co.kr. Accessed 10 Nov 2008
35. J.-B. Baek, C.B. Lyon, L.S. Tan, J. Mater. Chem. **14**, 2052 (2004). doi:10.1039/b401401d
36. K. Saeed, S.-Y. Park, H.-J. Lee, J.-B. Baek, W.-S. Huh, Polymer (Guildf) **47**, 8019 (2006). doi:10.1016/j.polymer.2006.09.012
37. Y.C. Ahn, S.K. Park, G.T. Kim, Y.J. Hwang, C.G. Lee, H.S. Shin, J.K. Lee, Curr. Appl. Phys. **6**, 1030 (2006). doi:10.1016/j.cap.2005.07.013
38. E. Pretsch, P. Buhlmann, C. Affolter, *Structure Determination of Organic Compounds Tables of Spectral Data* (Springer-Verlag, New York, 2000)
39. J.R. Bahr, J. Yang, D.V. Kosynkin, M.J. Bronikowski, R.E. Smally, J.M. Tour, J. Am. Chem. Soc. **123**, 6536 (2001). doi:10.1021/ja010462s
40. F. Pompeo, D.E. Resasco, Nano Lett. **2**, 369 (2002). doi:10.1021/nl015680y
41. Y. Di, S. Iannace, E.D. Maio, L. Nicolais, J. Polym. Sci. Pt. B Polym. Phys. **41**, 670 (2003)
42. P. Pötschke, M. Abdel-Goad, I. Alig, S. Dudkin, D. Lellinger, Polymer (Guildf) **45**, 8863 (2004). doi:10.1016/j.polymer.2004.10.040
43. C. Liu, J. Zhang, J. He, G. Hu, Polymer (Guildf) **44**, 7529 (2003). doi:10.1016/j.polymer.2003.09.013
44. Y. Dror, W. Salalha, R.L. Khalfin, Y. Cohen, A.L. Yarin, E. Zussman, Langmuir **19**, 7012 (2003). doi:10.1021/la034234i
45. J. Ayutsede, M. Ganghi, S. Sukigara, H. Ye, C.-M. Hsu, Y. Gogotsi, F. Ko, Biomacromolecules **7**, 208 (2006). doi:10.1021/bm0505888
46. R. Inai, M. Kotaki, S. Ramakrishna, J. Appl. Polym. Sci. Pt. B Polym. Phys. **43**, 3205 (2005). doi:10.1002/polb.20457
47. S.-Y. Park, Y.-H. Cho, R.A. Vaia, Macromolecules **38**, 1729 (2005). doi:10.1021/ma048258n
48. Y. Liu, L. Cui, F. Guan, Y. Gao, N.E. Hedin, L. Zhu, H. Fong, Macromolecules **40**, 6283 (2007). doi:10.1021/ma070039p